Thesis/
Reports
Catchpole,
E. A.

FINAL REPORT ON RJVA No. INT-91558 FY 1992

RESULTS OF LABORATORY FIRE BEHAVIOUR EXPERIMENTS

Coop Agreement
University of
New South
Wales

FINAL REPORT FOR RESEARCH JOINT VENTURE AGMT
#INT-91588-RJVA with
UNIVERSITY OF NEW SOUTH WALES
FS Contact: R. C. Rothermel
Co-op Contact: E. Catchpole

FINAL REPORT ON RJVA No. INT-91558

FY 1992

Results of Labortory Fire Behaviour Experiments

Experimental set-up

All the experiments were conducted in the large wind tunnel at the Intermountain Fire Sciences Laboratory (IFSL) in Missoula, Montana. The large wind tunnel at IFSL has been described by Anderson and Rothermel (1965). The test section has a 3.05 m $\times$ 3.05 m cross-section, and an overall length of 12.2 m. The fuel bed width used was 1 m. The bed lengths ranged from 5 m to 8 m, depending on the spread rate expected. The beds were placed on the floor of the tunnel, and had mesh sides 0.25 m high. Metal sheeting was placed along the mesh sides up to the height of the fuel. A spoiler screen of 0.25 m high mesh was placed in front of the fuel bed to initiate a turbulent boundary layer over the length of the fuel bed. This was supplemented by 0.0125 m mesh wire folded in Z-folds in front of the fuel bed, and also between the fuel bed and the tunnel walls. The height of the folds was the same as the fuel height.

A weighing platform was 0.93 m from the downwind end of the bed. It consisted of a fuel support platform 0.25 m long in the direction of propagation, and 0.40 m wide. The platform was perforated to equalise the pressure forces between top and bottom of the platform, and was supported by a center pedestal which went through the floor of the wind tunnel and onto the platform of an electronic balance.

The facility is capable of controlling air temperature and humidity as well as wind-speed, and tests were conducted at a range of temperatures and relative humidities. For fires burned in non-ambient conditions the fuel was pre-conditioned in a cabinet where temperature and humidity were set to produce the required equilibrium

moisture content. Conditions in the wind tunnel were set to the same levels before the fuel was brought in for assembly of the fuel bed and burning. Moisture contents ranged from 3% to 33%, although the majority of the fires were burned at ambient conditions. Wind velocity in the tunnel was controlled at levels ranging from 0.45 m/sec to 2.7 m/sec in the free stream above the boundary layer. The leading edge of the bed was ignited with a trough of ignition fluid consisting of 80% gasoline and 20% diesel fuel.

Sixteen photocells were arranged at 0.5 m intervals along the length of the fuel bed, 0.025 m above the surface of the bed, and pointing across the bed, in a direction perpendicular to the sides.

We used 5 different fuels to give a good range of surface-area to volume ratios, and to try to represent the range of fine to medium natural fuels. The fuels were (two sizes of excelsior: regular and coarse, ponderosa pine needles, and 6 mm square) sticks. Excelsior, or wood wool, consists of wood strands of uniform cross-section but variable length stripped from wooden boards and packaged in bales. It forms a random fuel array when distributed evenly over a fuel bed. The bulk density can be set by expanding or compressing the strands to the specified depth. Physical and chemical properties of these fuels are given in Table 1.

The excelsior and pine needles were distributed as uniformly as possible, loading adjacent areas of bed to a constant depth with a predetermined mass of fuel (Schuette 1965). The sticks were arranged vertically in drilled ceramic board using parallel rows of evenly spaced sticks. To produce a uniform packing ratio the sticks were in a triangular lattice arrangement when viewed from above (see Catchpole, Catchpole and Rothermel, accepted for publication in International Journal of Wildland Fire).

There were constraints on the combination of fuel and environmental variables

used, in that some combinations would not have sustained combustion, and some combinations would have been out of the range found in natural fuels. A full set of experiments using all combinations of fuel type, fuel depth, packing ratio and moisture content would also have been very time consuming. Our intention was to build a physical model rather than empirical model for firespread, and we concentrated on experiments that would increase our understanding of the physical mechanisms of fire spread, primarily the heat transfer process from the fire to the fuel ahead of the fire. We also avoided fires burning under marginal conditions, and used ranges of conditions that would be found in practice.

Results

Rate of spread and propagating flux

Our method of measuring spread rate improved over the experimental period. However, we always used a video back-up which was analysed by image analysis as described by McMahon *et al.* (1986). To be sure of the position of the fire front we placed string across the fuel bed at half-meter intervals and called out the arrival of the front at these strings, which was recorded on the audio track of the video tape. Initially, we also had someone record electronically when the front position was called out. This system was subject to observer error due to slow reaction time and parallax, and it was replaced by photocell estimation.

The photocells and their positioning are described in the previous section. A typical voltage output is shown in Figure 1. Unlike thermocouples the photocells have a reasonably sharp cut-off atthe end of the flaming zone. By comparison with the video and mass loss trace we determined voltages at which the onset and end of flaming combustion could be determined. Rate of spread was then estimated by a regression of distance versus time, after first omitting the first 3 observations (the first 1.5 m of spread), to make sure a steady state had been reached. As problems

sometimes arose with a particular photocell, cells with traces too far out from the normal were automatically rejected from the spread rate calculation.

As the number of combinations of variables involved was so large we had to cut down on replication, relying on fitting functions of the explanatory variables to give us an estimate of variability. However, for those fires where we had a good number of replicates, we found the variability in spread rates to be about $\pm 20\%$. Because of our interest in building a physically-based model, we first consider the effect of fuel and environmental variables on the propagating flux (Rothermel 1972).
The propagating flux is the summation of all the heat transfer processes from the flame to the fuel ahead of the fire required to bring the fuel to ignition and thus sustain the steady state rate of spread. From energy balance considerations, the propagating flux can be evaluated from the heat sink terms and the rate of spread

$$I_p = R\rho_b \epsilon Q_T, \quad w/m^2 \tag{1}$$

where R is the rate of spread, ρ_b is the fuel bulk density, mass of fuel per volume of fuel bed, ϵ is the effective heating number (Frandsen 1973) or the fraction of fuel initially brought to ignition, and Q_T is the heat of ignition (Wilson, 1990), replacing the heat of pre-ignition Q_{ig} (Rothermel 1972). Q_T may be approximated as a linear function of moisture content (Dunlap 1912), and can be estimated by

$$Q_T = Q_f + M_f Q_M \tag{2}$$

(Wilson 1985). Q_f varies weakly with fuel type. Values for typical forest fuels are given in Susott (1982).

Because our objective is to develop a model that will predict rate of spread, the propagating flux must be evaluated in terms of the major influences upon fire spread that are available prior to the fire. These would include both the fuel and environmental conditions. Ideally, these factors should be included in the model

through their influence on radiation and convective heat transfer, the physical forms of the propagating flux.

The primary environmental influences are windspeed and fuel moisture. Temperature and humidity are considered to make their influence felt through their effect upon fuel moisture content, although recent experiences with wild fires indicates that temperature or solar insolation may have a strong influence on flammability beyond that shown by fuel moisture. Fuel bed geometry can be arranged in an infinite variety of configurations. Primary attention was given to packing ratio, size, and depth. Fuel load is included as it influences packing ratio and depth. Mixtures of fuel sizes were also studied, but will require considerable further examination. Slope was not investigated, but will be included from other studies.

A primary effect of moisture on the propagating flux is to reduce flame temperature by the dilution of the volatilisation products (Albini 1980). In a homogeneous fuel bed this can happen in two ways. Firstly, the combustion interface in wind-aided fires is non-vertical, and moisture from the lower part of the bed may penetrate through while the upper layer of the bed is alight. Secondly, in fuels of larger diameter the outside of the fuel particle may be alight while moisture still remaining in the inside of the particle is being evaporated, and combining with combustion products.

Previously Rothermel and Anderson (1966) and Wilson (1990) burned zero-wind fires at varying moisture contents to determine the effect of moisture content on spread rate. Fig 2(a) and (b) show the propagating flux plotted against moisture content for some of our wind-aided fires. Rothermel and Anderson's needle data and Wilson's excelsior data for zero-wind data are shown as a comparison. In the case of loosely packed regular excelsior there seems to be little moisture damping for either zero-wind fires as Wilson (1990) found, or for low-wind fires. In fact, the propagating flux tends to *increase* slightly at higher moisture contents. For

the higher windspeed fires at low moisture contents there is some evidence of the propagating flux increasing with moisture content. There is a need for lower moisture content fires to investigate this relationship, but this is extremely difficult in practice.

For fires in pine needles it can be seen that the data lie on closely parallel lines on a log-linear scale. This shows that a similar relationship with moisture content holds for both zero-wind and wind-aided fires, and that the relationship is close to an exponential decay of the form

$$I_p = (I_p)_0 \exp(-kM_f). \tag{3}$$

Here $(I_p)_0$ is the zero-moisture content propagating flux, M_f is the moisture content, and k is a constant.

Plots showing the resulting effect of moisture content on rate of spread for excelsior and pine needles on a linear scale are given in Figures 2c and 2d.

Figure 3 shows that for a fixed windspeed the propagating flux (normalised to zero moisture content) has a strong dependence on $\sigma\beta$, where σ is the fuel particle surface-area to volume ratio, and β is the fuel bed packing ratio (volume of fuel per volume of fuel bed). $\sigma\beta$ is thus the surface-area of fuel per volume of fuel bed. The strong dependence on $\sigma\beta$ is to be expected, as both radiative and convective heat fluxes are strongly dependent on $\sigma\beta$. We found that for fixed windspeed $(I_p)_0$ was approximately proportional to $(\sigma\beta)^{\frac{1}{2}}$.

The relationship between propagating flux, and hence spread rate, with fuel bed depth appears complicated. The lightly packed regular excelsior fires showed a slight decrease in propagating flux with depth (see Figure 4a). The more heavily packed excelsior fires showed a greater decrease in propagating flux with depth (see Figure 4b). This same phenomenon is seen in the pine needle fires for which the packing ratio was similar or greater than that in the excelsior fires. This is shown

in Figure 4c. However, in our limited number of fires using 6 mm diameter sticks at a similar packing ratio to the heavily packed excelsior, the spread rate in 15 cm beds was about one and a half times that in 7.5 cm beds. Obviously the depth effect we are seeing is packing ratio dependent. Also the different orientation of the fuel particles may be having some effect on the heat transfer processes.

Figure 5 shows the effect of windspeed on spread rate for all fuels at a set of different packing ratios. Allowing for the slight effect of the difference in fuel bed depth these plots give an idea of the relative effects of windspeed, packing ratio and surface-area to volume ratio or fuel type on rate of spread.

Note the relatively high spread rate at a windspeed of 0.9 m/sec for the 0.005 packing ratio excelsior fires. This was typical of the faster spreading fires burned at this windspeed. More details of this phenomena are given later. In the later experiments we avoided this windspeed. But, because of this problem, and because the wind tunnel speed is restricted to less than 3 m/sec, we prefer not to draw any conclusions as to the form of the relationship between spread rate and windspeed from our laboratory data.

Reaction time

The photocells gave us a good method of measuring the flaming combustion time which, following Rothermel 1972 we refer to as 'reaction time'. Reaction time was used to estimate fireline intensity and reaction intensity as discussed below. It is also an
important measure in determining fire temperature history for gauging fire effects.

Reaction time was estimated as the average time between the onset and end of flaming combustion for all working photocells. Results from this method correlated closely with reaction times estimated by flame depth divided by spread rate from

the video analysis. However, when the flame depth was large, and out of range of the video, the photocell method gave better results. The video analysis was also more prone to observer bias.

We found that reaction time was independent of windspeed in wind-aided fires (see Figure 6, for example). The reaction times also were comparable to, but possibly a bit higher than, the reaction times estimated by Wilson (1990) for the corresponding zero wind fires (see Figure 6). Wilson used flame depth divided by spread rate, but estimated flame depth visually.

Reaction time increased with moisture content, independently of windspeed, in the pine needles and excelsior where the effect of varying moisture content were tested (see, for example, Figure 7). The increase appears reasonably linear.

While the effect of varying fuel packing ratio and loading was quite pronounced, the effect of varying fuel type and hence the surface-area to volume ratio was not significant. It was found that reaction time, τ_r, was proportional to $\beta\delta^{0.6}$. The lack of relationship between τ_r and σ is contrary to previous findings in the zero-wind case (Anderson 1969, Wilson 1990). It is not yet known whether this is due to differences in fuel type and orientation, or whether it is a genuine property of reaction time for wind-aided fires.

Efficiency

Efficiency, as defined by Rothermel (1972), is the fraction of the dry fuel loading consumed in the flaming zone. We used efficiency to estimate the Byram's intensity and the reaction intensity, as described below.

Efficiency was obtained from the mass loss trace which was output from the weigh-

ing system. A typical mass loss trace, overlaid with the photocell response is shown in Figure 1. We found that the onset of flaming defined by the photocell response tended to be just prior to the sharp drop in mass loss. This is probably because not all fuel across the length of the slot is burning initially. So we formulated an algorithm to determine t_1, the beginning of the sharp drop in mass loss, and then used the reaction time, determined above, to estimate the end of flaming combustion t_2. The algorithm to determine t_1 essentially finds the intersection of the horizontal line through the average initial mass on the weighing platform with the regression line through the first third of the mass loss curve (see Figure 8). We then determined the masses m_1 and m_2 corresponding to these two time points. Dividing $m_1 - m_2$ by the initial dry mass on the weighing platform then gives the efficiency η_δ.

Efficiency was not related to packing ratio, fuel depth or windspeed. It did change for different fuels, but this seemed to be related to fuel type rather than fuel size. In ambient conditions the efficiency of the two excelsior fuels averaged 0.9, the efficiency of pine needles averaged 0.8, and 6 mm sticks averaged 0.7.

There might be a slight decrease in efficiency with moisture content for the pine needle fires, but no relationship could be seen for the excelsior fires. The primary differences in efficiency in our data set appear to be fuel-type related.

Byram's intensity

Byram's intensity, or the fireline intensity, is the rate of heat release per unit length of fireline (Brown and Davies 1963). It can be used to estimate flame length (Brown and Davis 1963), suppression difficulty (Roussopoulos and Johnson (1973), 'blow-up conditions' (Rothermel 1990) and severity of fire effects (Chandler *et al.* 1983). Byram's intensity I_B is estimated from

$$I_B = hw_aR, \tag{4}$$

where h is the heat content of the fuel, and w_a is the 'available fuel', or fuel consumption. As we were primarily interested in developing a fire behaviour model, rather than estimating fire effects, we considered w_a to be the fuel consumption in the flaming zone. So we estimated w_a from $w_0\eta_\delta$, where w_0 was the dry fuel loading. From the same consideration we followed Wilson (1990) and used h_v, the heat of volatisation, the heat given out during flaming combustion, rather than the total heat content. h_v is the total heat content with the heat content of the char subtracted. Values for different forest fires are given in Susott (1982). As we use the heat of volatilisation and the fuel consumed in the flaming zone, the moisture content corrections to the heat of consumption described in Brown and Davies (1963) are not necessary. Hence we estimated the fireline intensity as

$$I_B = h_v w_0 \eta_\delta R. \tag{5}$$

Fireline intensity is obviously a function of fuel and environmental parameters through R,and η_δ, so it is not necessary to discuss the explicit behaviour of I_B with fuel and environment.

Reaction intensity

Reaction intensity is the heat flux per unit horizontal area of the combustion zone. It was used by Rothermel (1972) as a source term for the heat transfer, and by Thomas (1962,1967) and Albini (1981) to model flame properties. The reaction intensity at any time t, $I_R(t)$ is proportional to the instantaneous mass loss rate per unit area, i.e.,

$$I_R(t) = h\frac{dw}{dt}, \tag{6}$$

where w is the fuel loading. Differentiating the mass loss curve, as shown in Figure 1, multiplying by the heat content and dividing by the weighing platform area, gives the reaction intensity as a function of time. For fine fuel the reaction intensity tends to peak close to the fire front (Frandsen and Rothermel 1972), whereas for 6 mm

sticks the reaction intensity has a long flat peak at the center of the combustion zone (see Figure 1).

The method of estimating reaction intensity depends on the longitudinal depth of the weighing platform relative to the longitudinal depth of the combustion zone (Frandsen and Rothermel 1972), so our method differs from the methods used by Rothermel (1972) and Wilson (1990) who were burning zero-wind fires with a large platform width. For our fires the combustion zone depth was large compared to the platform depth.

We used two estimates of reaction intensity, I_{Rmax}, which was the maximum reaction intensity recorded, and I_{Rave}, which was the average reaction intensity during the reaction time. Estimating I_{Rmax} presented many problems. The numerical derivative of the mass loss curve was unstable when bumps or notches appeared in the mass loss curve. These were often due to a falling piece of fuel. We tried using the average reaction intensity over the first third of the curve to estimate I_{Rmax}, but this could be badly affected by a bad estimate of the initiation of mass loss. We found that I_{Rave} was a much more robust property of the mass loss curve to estimate.

Our estimate of I_{Rave} was

$$I_{Rave} = h_v w_a \tau_r, \tag{7}$$

where h_v was used for reasons explained above, and w_a and τ_r were estimated as described above.

I_{Rave} for our regular excelsior fires was found to be lower than the reaction intensity Wilson (1990) estimated for the corresponding zero-wind fires (see Figure 9), but this may relate to different measurment techniques. Rothermel and Anderson (1966) also found the reaction intensity in the wind-aided case was lower than in the zero-wind case, but the same reason may apply. Apart from this, reaction

intensity appears virtually unaffected by windspeed, although there may be a slight decrease at higher windspeeds.

To model the effect of moisture content on reaction intensity Rothermel (1972) defined a 'moisture damping coefficient' η_M such that

$$I_R = (I_R)_0 \eta_M, \tag{8}$$

where $(I_R)_0$ was the zero-moisture reaction intensity. Rothermel used a cubic function of moisture content for η_M. Wilson (1990) burned many more zero-wind fires at varying moisture contents, and found that an exponential damping coefficient of the form.

$$\eta_M = \exp\left(-\frac{M_f}{M_\sigma}\right) \tag{9}$$

was the best fit to his data. The 'characteristic moisture content' M_σ was a function of surface-area to volume ratio and fuel type.

The damping in our wind-aided fires is slightly greater than in Wilson's zero-wind fires, as shown in Figure 10, which is plotted on a log-linear scale. This means that the constants in Wilson's formula for η_M probably need slight modifications for use in wind-aided fires.

Wilson developed a formula relating reaction intensity to packing ratio, fuel depth and surface-area to volume ratio. We tried develop a similar functional form of σ, β and δ, but found again that surface-area to volume ratio was not a significant variable. Again this may relate to differences in fuel type and orientation. We fitted the following equation to our estimated average reaction intensity

$$I_{Rave} = k\, h_v\, w_0 \Gamma \eta_M, \tag{10}$$

where $k = 0.00073$, and the reaction velocity Γ (Rothermel 1972) is given by

$$\Gamma = (\beta\delta)^{-0.63} \exp(-15.2\beta), \tag{11}$$

where all measurements are in SI units, and δ is the fuel bed depth. Note firstly that this is a similar functional form in β and δ to that given by Wilson (1990),

and secondly that the loading $w_0 = \rho_p \beta \delta$, where ρ_p is the fuel particle density. The observed and fitted values are plotted in Figure 11, the correlation coefficient r being equal to 0.68.

Flame Dimensions

Flame dimensions were measured using the video image analysis system. Flame length has been used as an alternative to Byram's intensity to describe supression difficulty (Alexander 1989), flame height is important in determining scorch height for fire effects purposes (Gill 1988), and knowledge of both flame length and flame angle are important in determining the amount of radiative heat transfer Albini (1985). Because flame height can be determined as $L \cos\theta$ (where L is the flame length, and θ the flame angle from the vertical) we confine our discussion to results about flame length and angle.

We first make it clear that we measured flame length parallel to the paths of the buoyant particles, and the flame angle was the angle between the measured flame length line and the vertical. This method was also used by Nelson and Adkins (1986). However, Byram developed a relationship between fireline intensity and flame length, for which the flame length was measured from the midpoint of the combustion zone to the flame tip (Nelson, personal communication).

We found that our flame length increased very little, if at all, as windspeed increased. Nelson and Adkins (1986) found that for their laboratory needle fires that flame length was independent of Byram's intensity, but as their loadings and moisture contents remained virtually constant, so that Byram's intensity varied primarily with windspeed. this result is consistent with ours. If we had used Byram's definition of flame length then flame length would have increased with windspeed because of its strong correlation with flame depth which is highly windspeed dependent.

Flame length did, however, increase with Byram's intensity when the loading was increased. It had a strong correlation with Byram's intensity ($r = 0.66$) which dropped off at higher intensities. Flame length was also strongly correlated with reaction intensity ($r = 0.69$). However, by far the most strongly correlated single variable was fuel depth ($r = 0.70$). See Figure 12 for plots of these variables against flame length.

We found that flame angle could be closely related to the 'Byram's number', the power of the fire divided by the power of the wind (Brown and Davies 1963), a concept used by Byram to decide which heat transfer effects dominated a fire (see Figure 13). The power of the fire is proportional to the Byram's intensity, whereas the power of the wind is proportional to the cube of the difference between windspeed and spread rate.
The relationship, however, became less strong for larger values of Byram's number. A similar correlation was observed by Martin *et al.* (1991), but note that they use the flame angle from the horizontal.

Models for fire behaviour

Anderson's equation for residence time
There has been some confusion in the literature between the terms 'residence time' and 'reaction time', so we have in this paper reserved 'residence' time for the time it takes a single fuel particle to burn out. Anderson's formula, given in Anderson (1969) thus actually predicted what we have called 'reaction time'. This formula predicted reaction time in terms of surface-area to volume ratio only, although Anderson noted that packing ratio also had an effect. As can be seen from our experiments in the wind-aided fires, packing ratio, depth and moisture content are the main variables which affect reaction time. Until we are sure that surface-area to volume ratio has no effect on reaction time we prefer not to present an alternative formula for reaction time. Some extra experimentation will be carried out to test directly the effect of surface-area to volume ratio.

The Rothermel model for rate of spread

The model presented by Rothermel (1972) for predicting rate of spread from fuel and environmental variables, has been widely used around the world. It is the backbone of the BEHAVE computer system for predicting fire behaviour (Burgan and Rothermel (1984), Andrews 1986, Andrews and Chase 1989). The philosophy of the model is that the horizontal propagating flux is a fraction of the vertical reaction intensity, and that fraction can be expressed in terms of fuel geometry parameters.

We do not attempt to fit the Rothermel model to our data because we are aware of problems with the original model, and we are engaged in building a second generation model which will more closely reflect the underlying heat transfer processes. One of the problems is the original model's over-sensitivity to fuel depth (Gould 1990). The assumption of proportionality between the propagating flux and reaction intensity resulted in the assumption that the propagating flux increased proportionally with depth through its effect on loading. Since the original experiments were done at one fuel depth for each fuel type, this assumption was not previously tested.

Wilson (1990) did many zero-wind experiments in fuel of varying depth. His results show that spread rate in zero-wind is proportional to the square root of depth—a weaker depth dependence than originally assumed. It seems, however, in wind-aided fires that the dependence on depth is more complicated, and depends on the fuel type and geometry. This is probably reflecting differences in the heat transfer processes.

The Carrier, Fendell, Wolff model for rate of spread

From dimensional analysis and wind tunnel testing Carrier *et al.* (1990) developed a model for rate of spread of the form

$$R = k\left(\frac{U}{w_0}\right)^{\frac{1}{2}}, \tag{13}$$

where w_0 is the dry fuel loading, U is the ambient windspeed, and k is a constant. This model applies to ambient conditions and *fixed* fuel depth. This implies that increases in w_0 are due to increases in bulk density assuming particle density is virtually constant.

Thus the bulk density relationship obtained by Carrier *et al.* is the same as ours, since we found the propagating flux I_p to be proportional to $\beta^{\frac{1}{2}}$. Since $R = \frac{I_p}{\rho_p \beta \epsilon Q_T}$, we get R proportional to $(\frac{1}{\beta})^{-\frac{1}{2}}$.

The relationship between spread rate and windspeed for our data is confused by the low windspeed phenomena (to be discussed in the next section). However, from data not affected by this low windspeed problem it appears that the relationship we obtained between spread rate and windspeed is stronger than the one given by Carrier *et al.* (see Figure 5), and at least linear rather than concave downward.

In the second part of their paper Wolfe *et al.* (1990) give a tentative relationship between spread rate and windspeed that takes into account varying fuel depth in their experiments. This relationship is

$$R = k\left(\frac{U}{w}\right)^{\frac{1}{2}}\left(\frac{\delta}{d}\right)^{\frac{2}{3}}, \tag{14}$$

where d is the fuel diameter, and k is a constant. So, for fixed bulk density Wolfe *et al.* have spread rate proportional to $\delta^{\frac{1}{6}}$, where δ is fuel depth. This is a very weak dependence on fuel depth. Their fuels were principally vertical sticks with

dimensions between our coarse excelsior in which the depth versus spread rate correlation was slightly negative, and our 6 mm sticks for which spread rate was proportional to $\delta^{\frac{3}{2}}$. The depth relationship given by Wolfe *et al* may therefore be representative of an intermediate fuel diameter range.

For cylindrical fuels the surface-area to volume ratio can be approximated by $4/d$, where d is the fuel diameter. So the relationship between rate of spread and diameter in (14) implies that spread rate is approximately proportional to $d^{\frac{2}{3}}$ rather than $d^{\frac{1}{2}}$ as we obtained. However, Wolfe *et al.* forced a relationship of the form $\frac{\delta}{d}$ from dimensional considerations, so that their fuel diameter relationship is not necessarily the one that least-squares fitting would have produced.

Nelson and Adkin's model

Nelson and Adkin (1986) developed a model for rate of spread from dimensionless correlation arguments and the combination of several laboratory and field data sets. The model is not predictive as it gives a formula for spread rate in terms of fire behaviour variables rather than variables that can be measured prior to a fire. However, as we have good measurements of the fire behaviour variables required it is worth testing the model against our data.

The formula given for spread rate (in SI units) is

$$R = 0.39\, w_a^{0.25}\, U^{1.51}/\tau_r,$$

where U is the ambient windspeed. Because of our low-wind recirculation problem we removed fires affected by this problem (fires with windspeeds of 0.9 m/sec) from the data set, and fitted the model to the remainder of the data. Results are given in Figure 14. The model badly undepredicted the rate of spread, especially for the finest fuels. If the constant in the model is doubled a better fit results, but there is still considerable scatter.

Discussion

Flame length

The result that flame length does not increase with windspeed in our experiments is somewhat surprising. Because we measured flame length in a different way to some other fire researchers we cannot directly compare our results with the results that some others have found. It is possible that it is a phenomena associated with closed wind tunnel combustion. We did take pains to watch out for the 'choking' described by Nelson and Adkins (1986) that they thought might be present in their higher intensity fires. We observed no flame bending near the ceiling of the tunnel, and the pitot tube measuring free stream velocity 3, showed constant wind velocity whereas choking would cause a reduction in velocity.

Velocity profiles taken prior to the fire with a hot film anemometer showed a typical logarithmic profile from a turbulent boundary layer up to about 80 cm from the floor. Possibly the boundary layer is too shallow to be representative of external conditions, and the flame length is being curtailed by the ambient laminar flow above the boundary. However, confirmation is needed from other sources to determine whether this is a closed tunnel phenomena or whether it occurs in other situations.

Low windspeed problem

We initially conducted our fire experiments at windspeeds of 0.9, 1.8 and 2.7 m/sec (2, 4 and 6 mph), the highest of these being the maximum achievable in the tunnel at present. We noticed the spread rates at 0.9 m/sec, particularly in the regular excelsior at the lower packing ratios, were similar to the spread rates at 1.8 m/sec. Burning at 0.45 m/sec confirmed that the 0.9 m/sec spread rate was anomalous (see Figure 5).

A hot-wire anemometer on the roof of the tunnel showed severe fluctuations during these 0.9 m/sec fires, whereas it remained stable at faster windspeeds. We put a smoke generator close to the roof of the tunnel and light tinsel strands at various levels in the tunnel. From this it could be observed that there was a strong back circulation of flow close to the tunnel roof which started at the fire front, flowed back several meters to the tunnel entrance and reversed, to flow downwards and forward toward the fire. A similar back flow was also seen at a windspeed of 0.45 m/sec, but very much reduced. There was no back flow at 1.8 m/sec.

It may be that the back flow is acting to increase the spread rate of fires with windspeeds of around 0.9 m/sec. Another explanation is a change in flow regimes such as a change from laminar to turbulent flow which Viegas and Neto (1990) attribute to the sudden change in the relationship between spread rate and shear stress that they noted.

After discovering the back circulation we avoided this windspeed. We confined our testing of the effect of fuel variables and moisture content to 1.8 and 2.7 m/sec, and used 0.45 m/sec if a low windspeed fire was necessary.

Further work

As previously emphasised our primary concern is to get a model for firespread that describes as closely as possible the physical process of heat transfer that is occurring in free-burning fires. We have already burned about 250 experimental fires in homogeneous fuel beds to develop our model. We have improved our instrumention over a period of years, and are now measuring fuel and air temperature profiles, surface windspeed, friction velocity and radiative flux on each fire. These measurements should give us more insight into the determining factors influencing firespread. During this investigation we also hope to look closely at the effect of

shear stress which Viegas and Neto (1990, 1991) argue should be important in influencing the rate of heat transfer.

Apart from fires in homogeneous fuels we have investigated firespread in combinations of mixed diameter fuels (Catchpole, Catchpole and Rothermel, submitted). In the near future we hope to continue this mixed fuel program of burning, to try and model firespread in the complex fuel arrays which occur in natural vegetation.

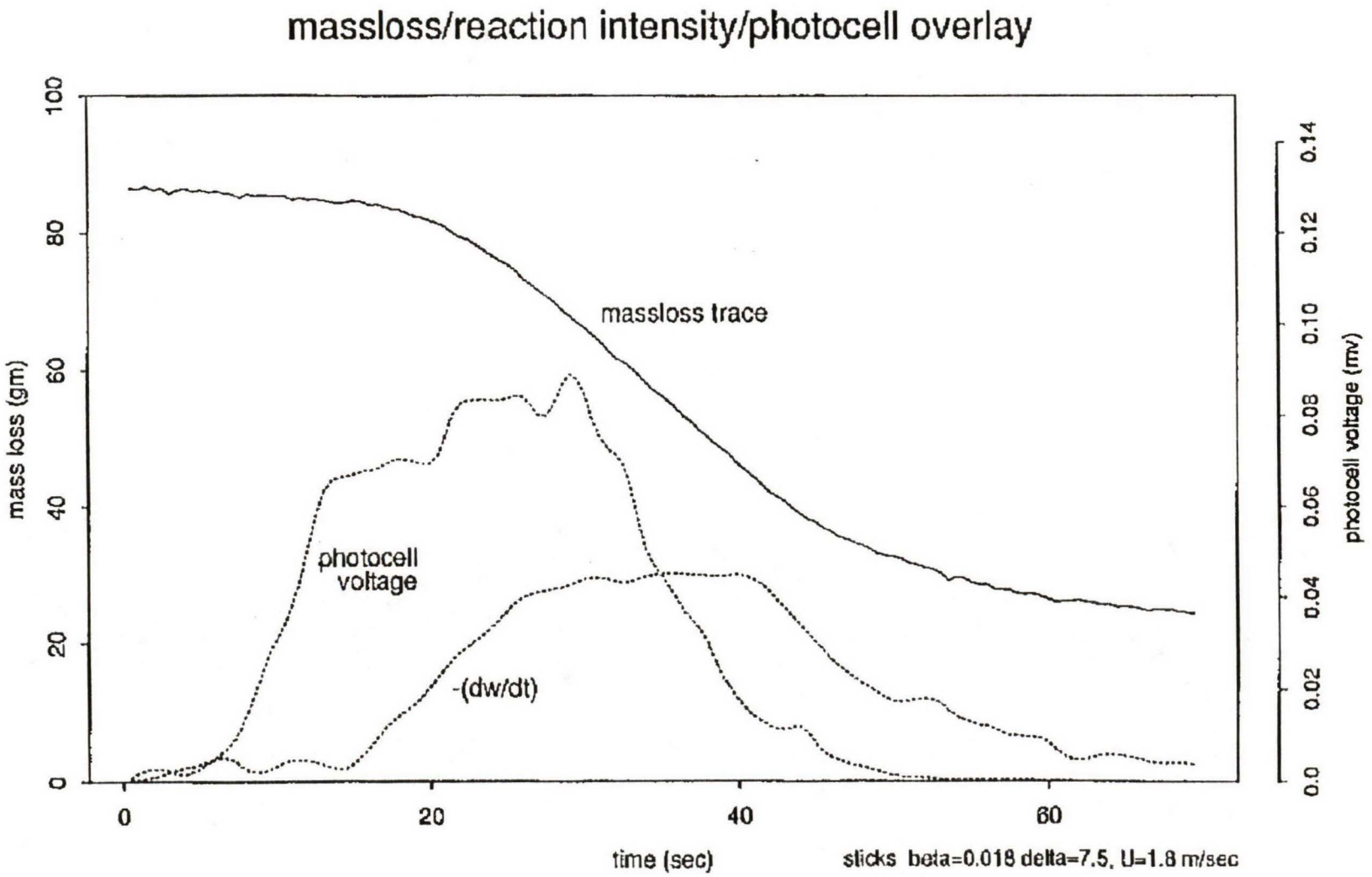
massloss/reaction intensity/photocell overlay
mass loss (gm)
photocell voltage (mv)
massloss trace
photocell voltage
-(dw/dt)
time (sec)
sticks beta=0.018 delta=7.5, U=1.8 m/sec
0
20
40
60
80
100
0.0
0.02
0.04
0.06
0.08
0.10
0.12
0.14

Figure 1

Regular excelsior: propagating flux versus moisture content

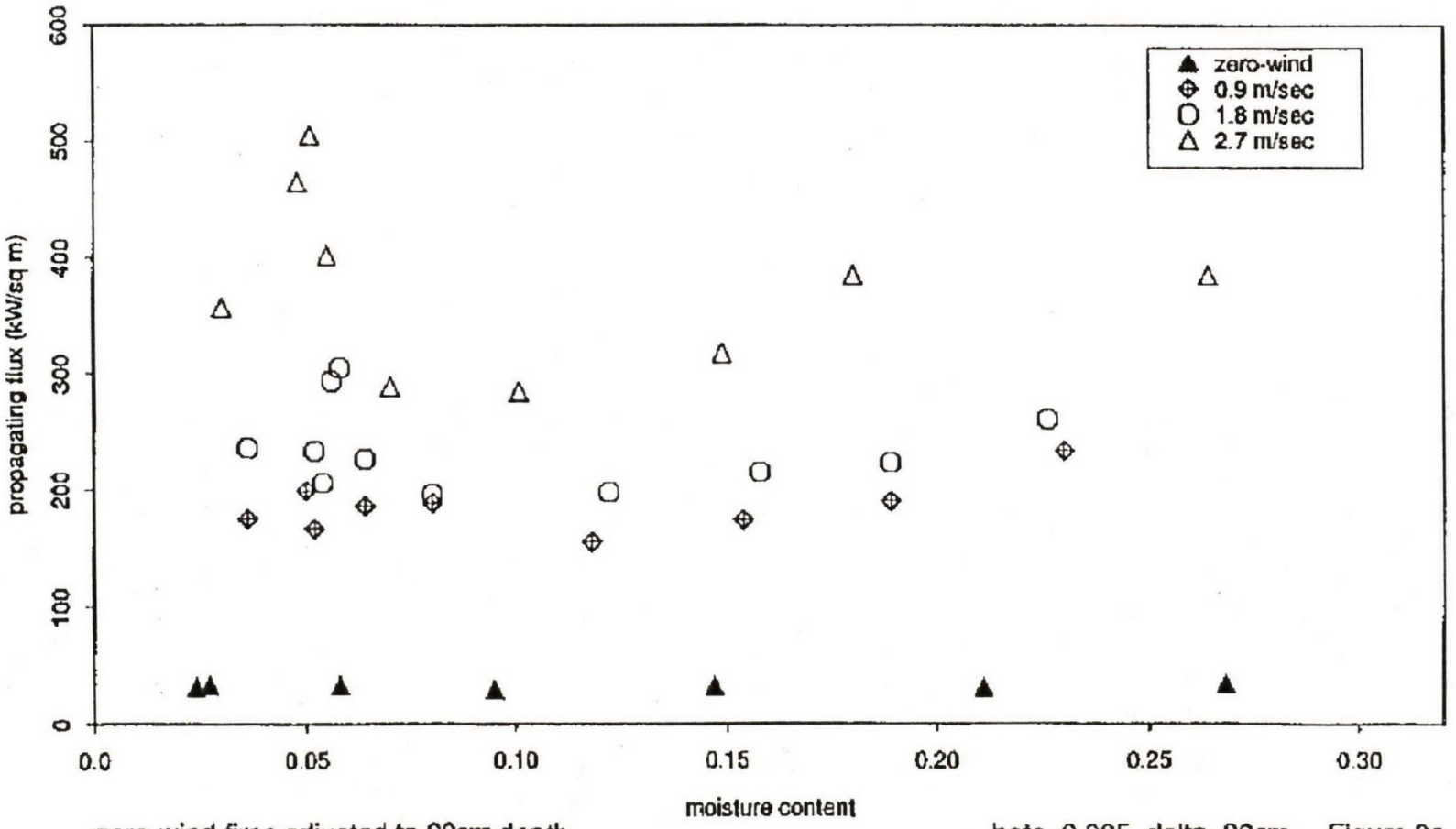

zero-wind fires adjusted to 20cm depth

beta=0.005, delta=20cm Figure 2a

Pine needles: propagating flux versus moisture content

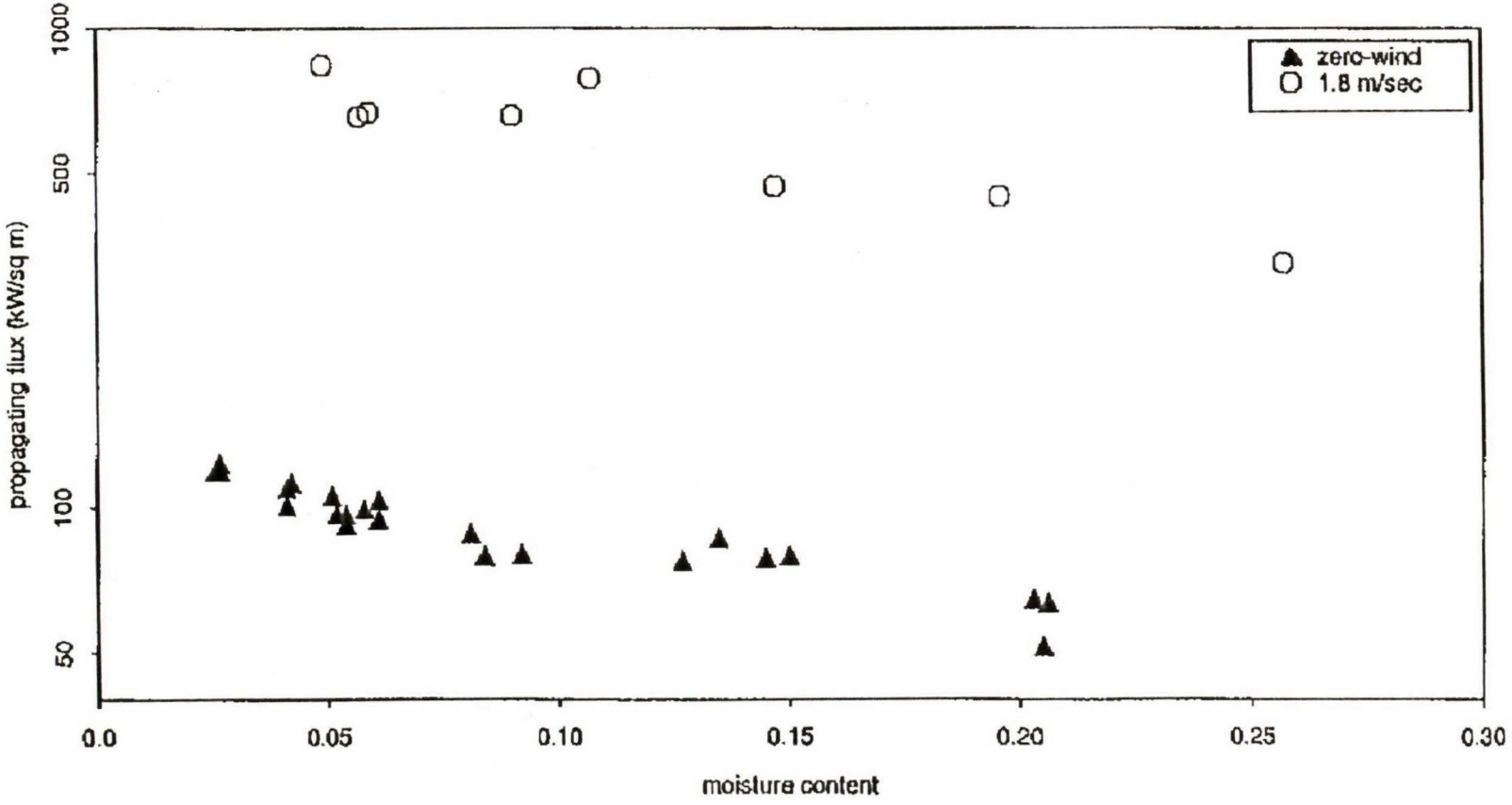

delta= 7cm (zero-wind), delta=2.5 cm (wind-aided), beta=0.065

Figure 2b

Regular excelsior: rate of spread versus moisture content

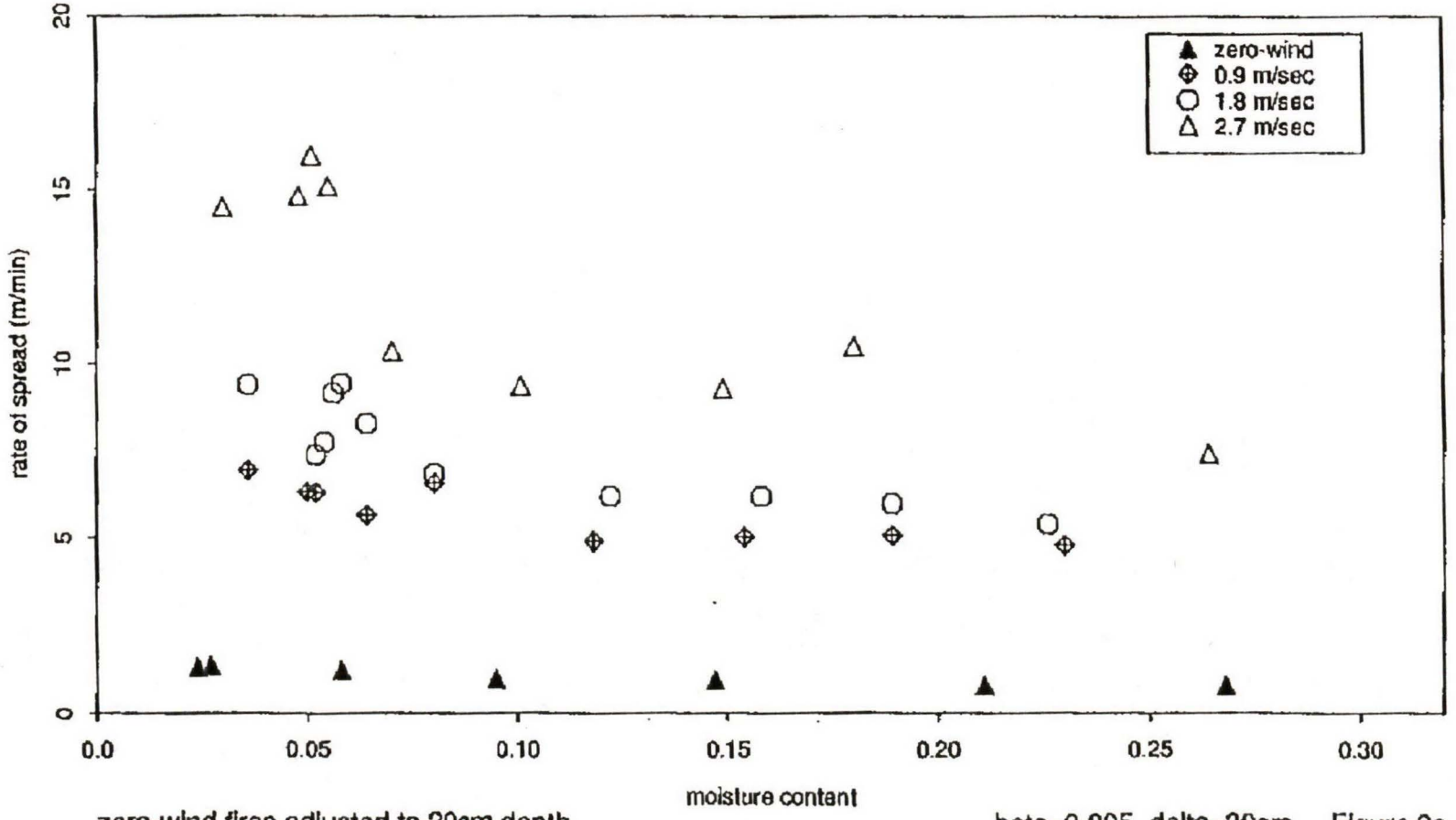

zero-wind fires adjusted to 20cm depth

beta=0.005, delta=20cm Figure 2c

Pine needles: rate of spread versus moisture content

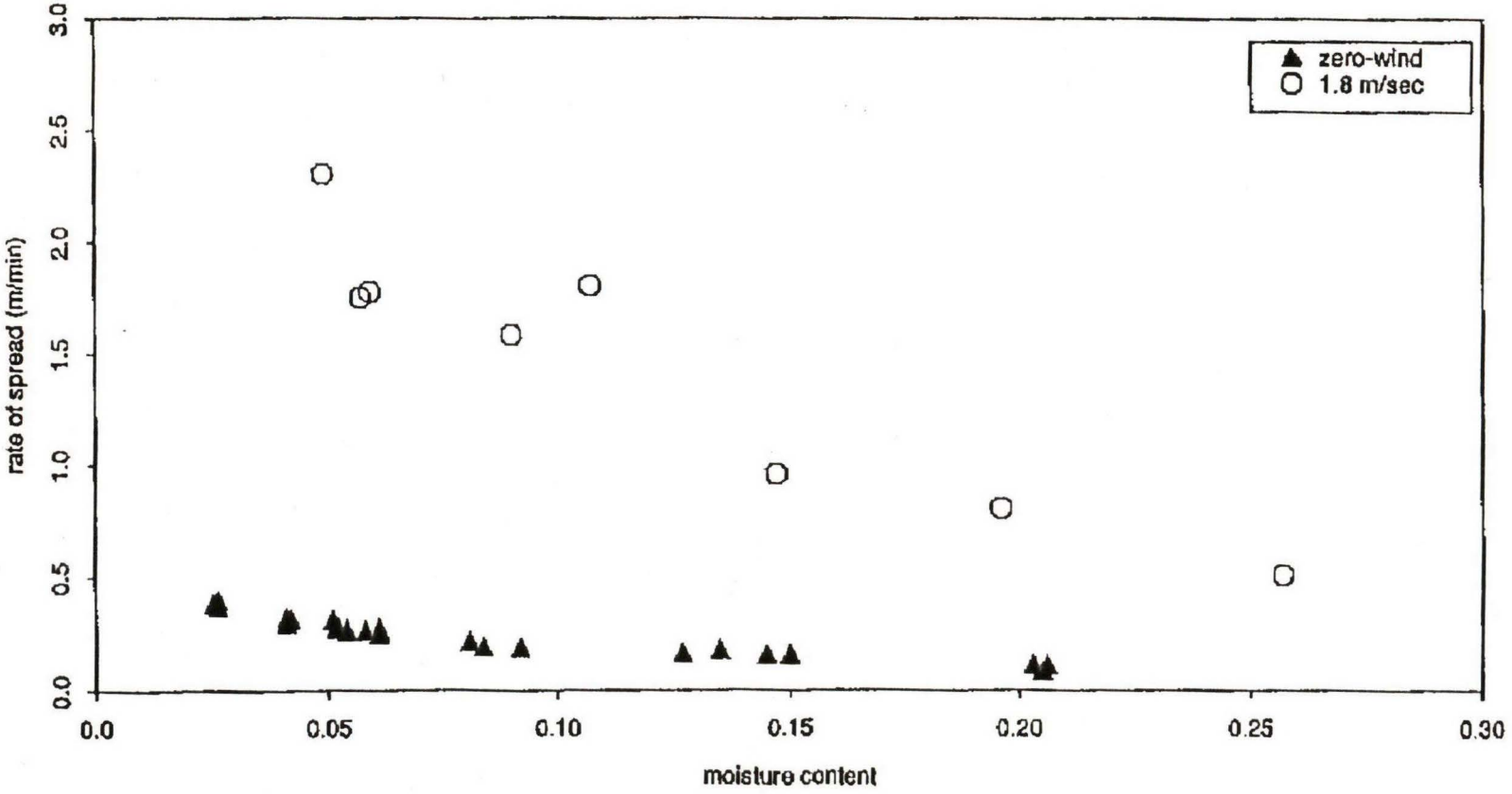

delta= 7cm (zero-wind), delta=2.5 cm (wind-aided), beta=0.065

Figure 2d

Propagating flux versus sigma*beta

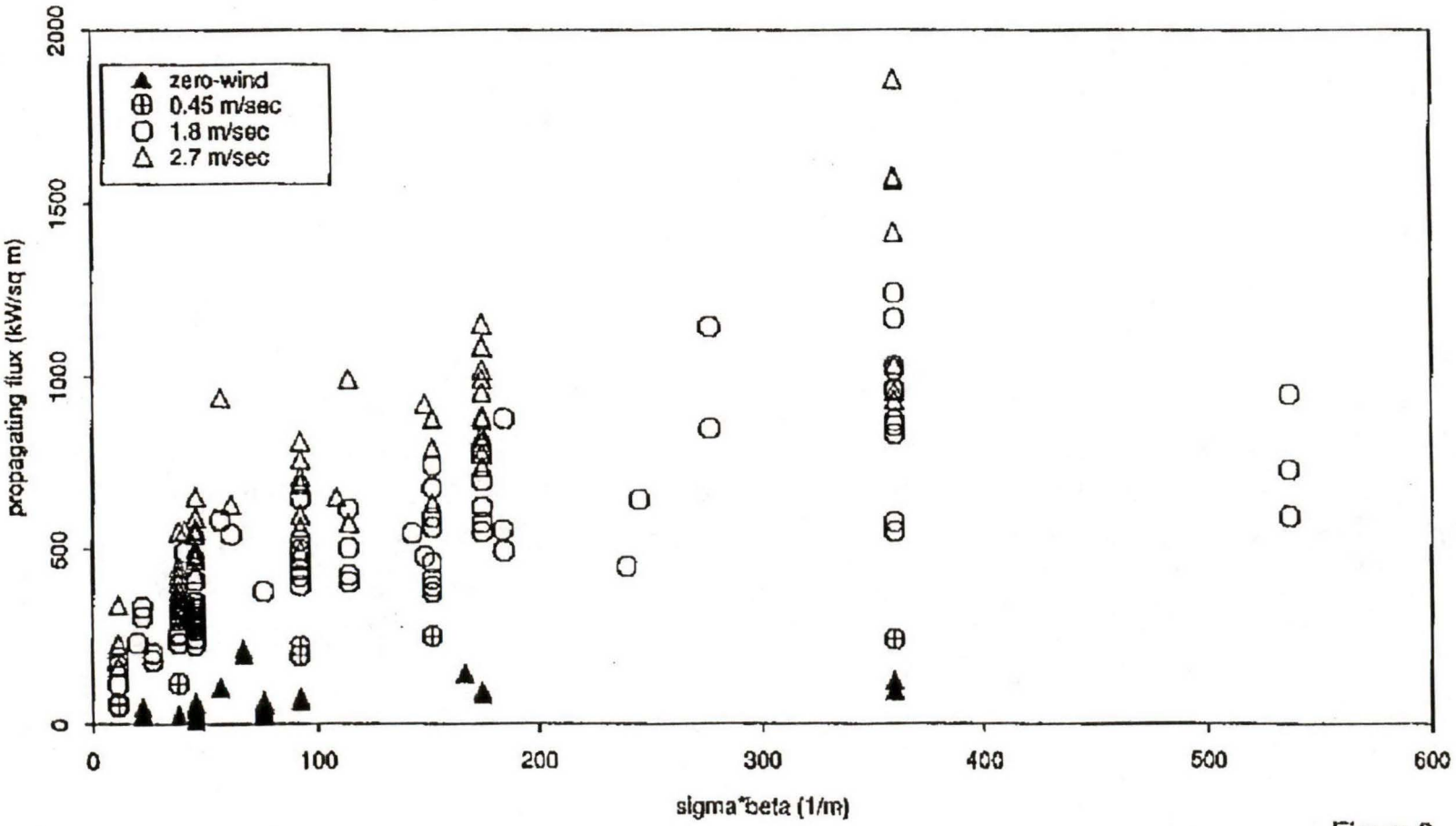

Figure 3

Excelsior, beta=0.005: propagating flux versus depth

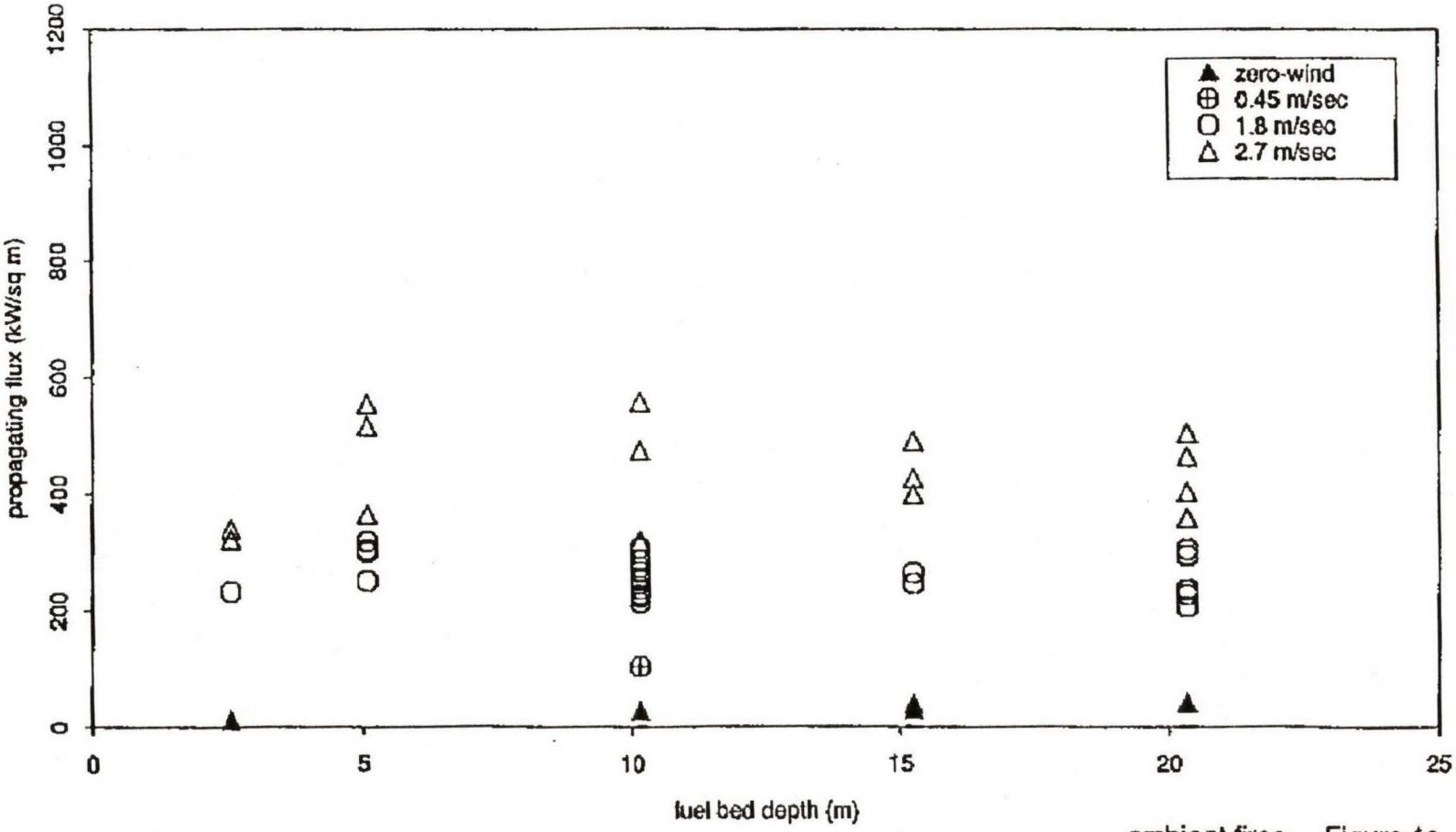

ambient fires Figure 4a

Excelsior, beta=0.02: propagating flux versus depth

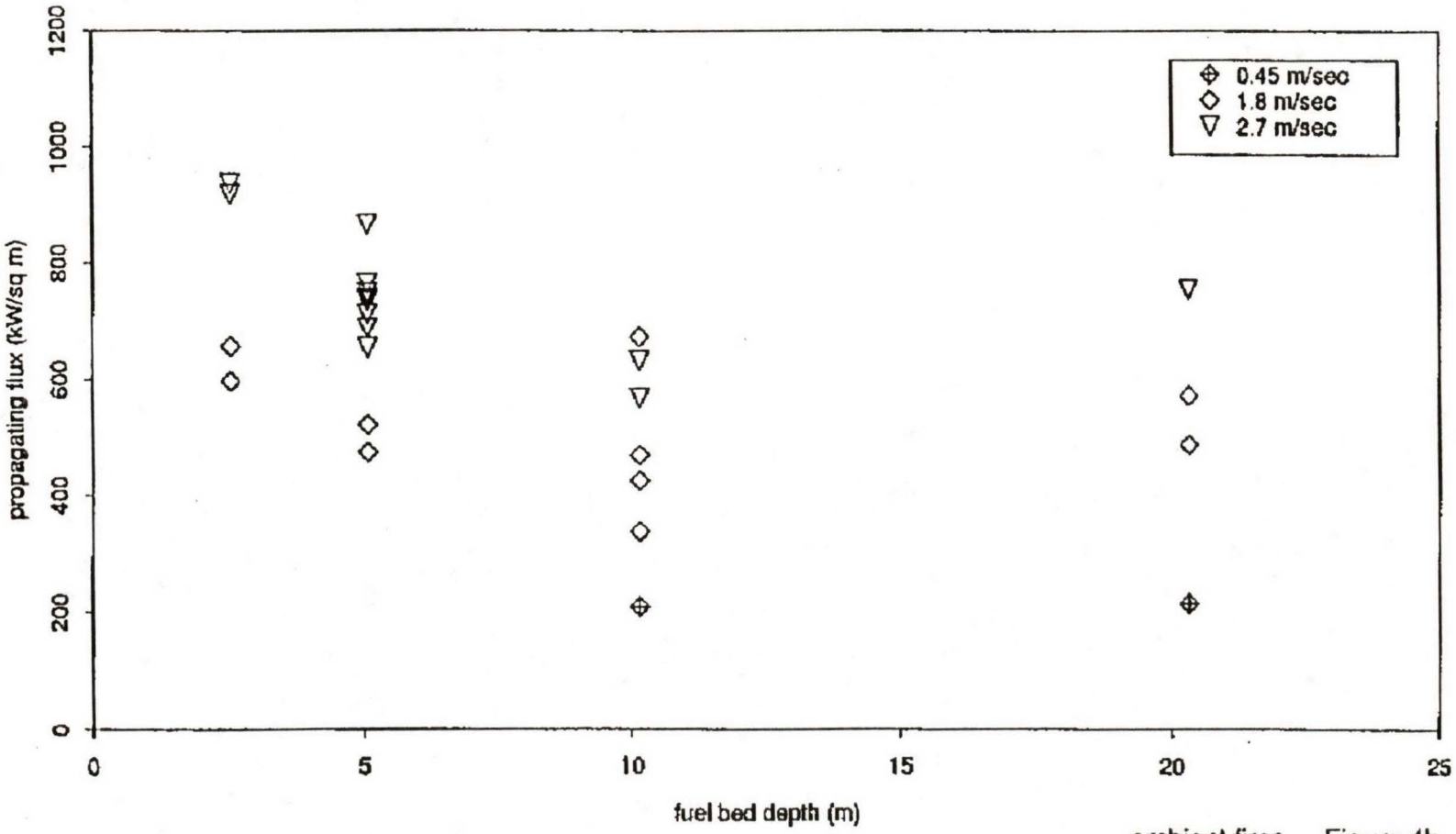

ambient fires Figure 4b

Pine needles: propagating flux versus depth

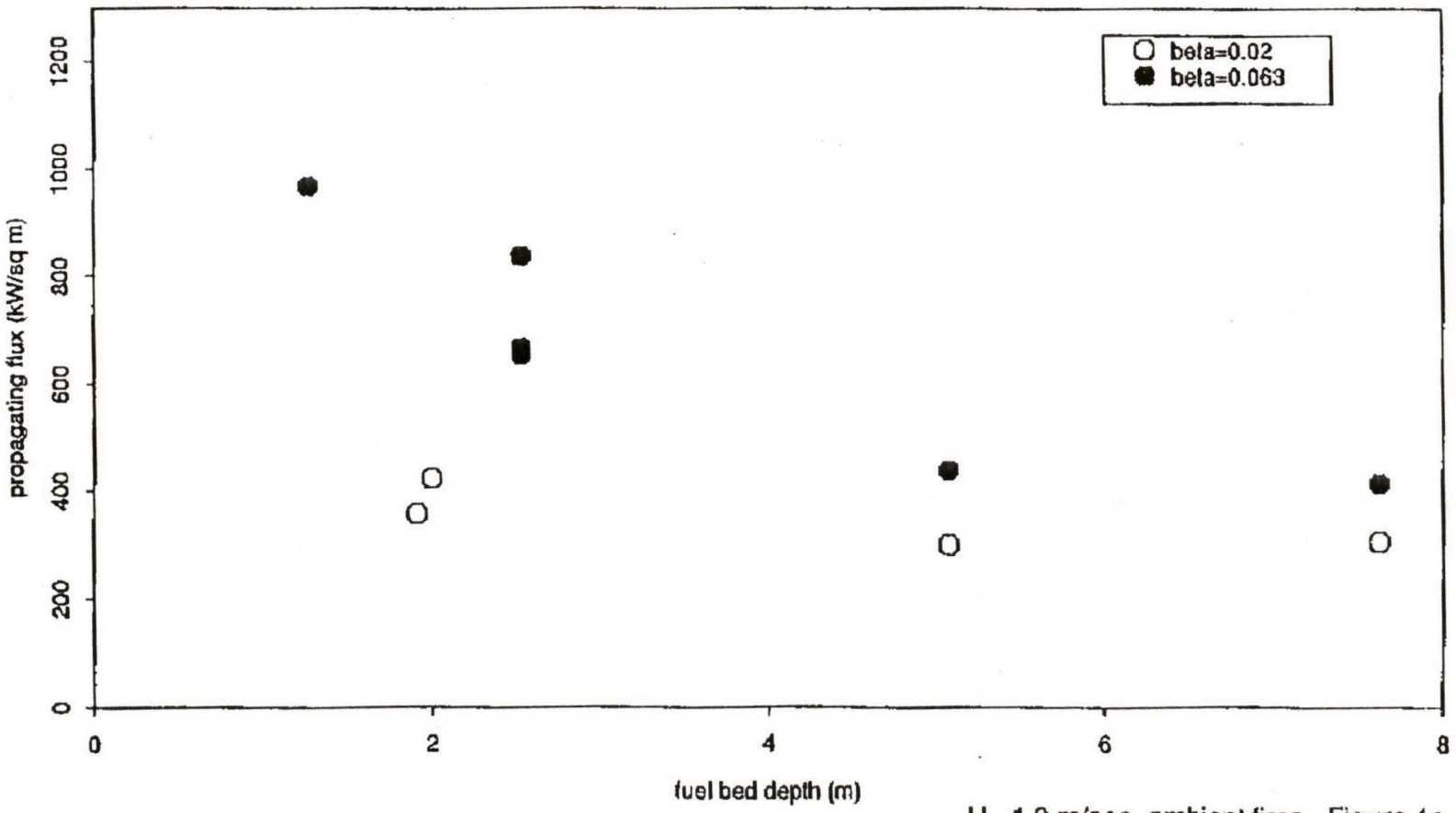

U= 1.8 m/sec, ambient fires Figure 4c

Spread rate versus windspeed - ambient conditions

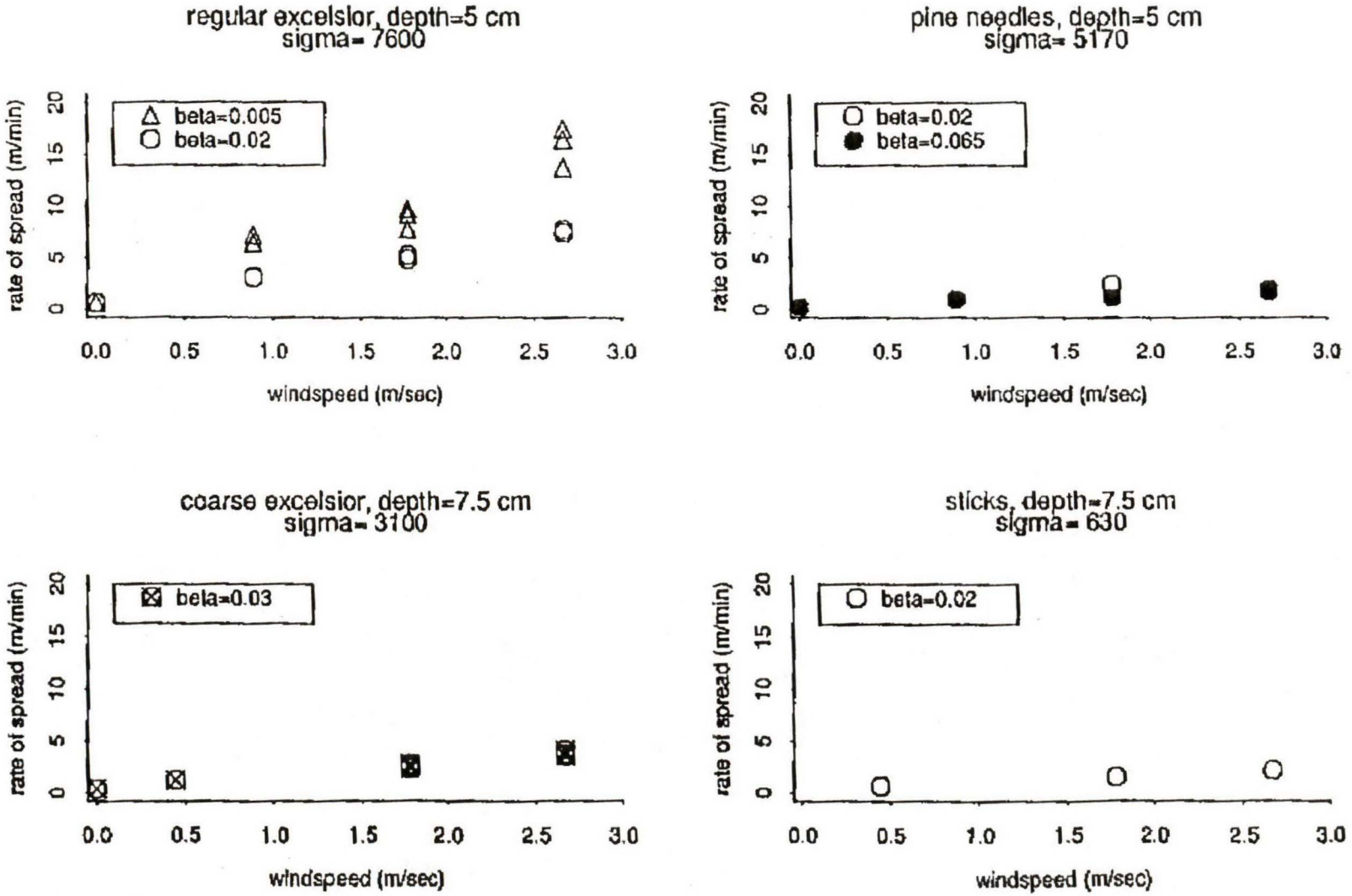

Figure 5

Reaction time versus windspeed - ambient conditions

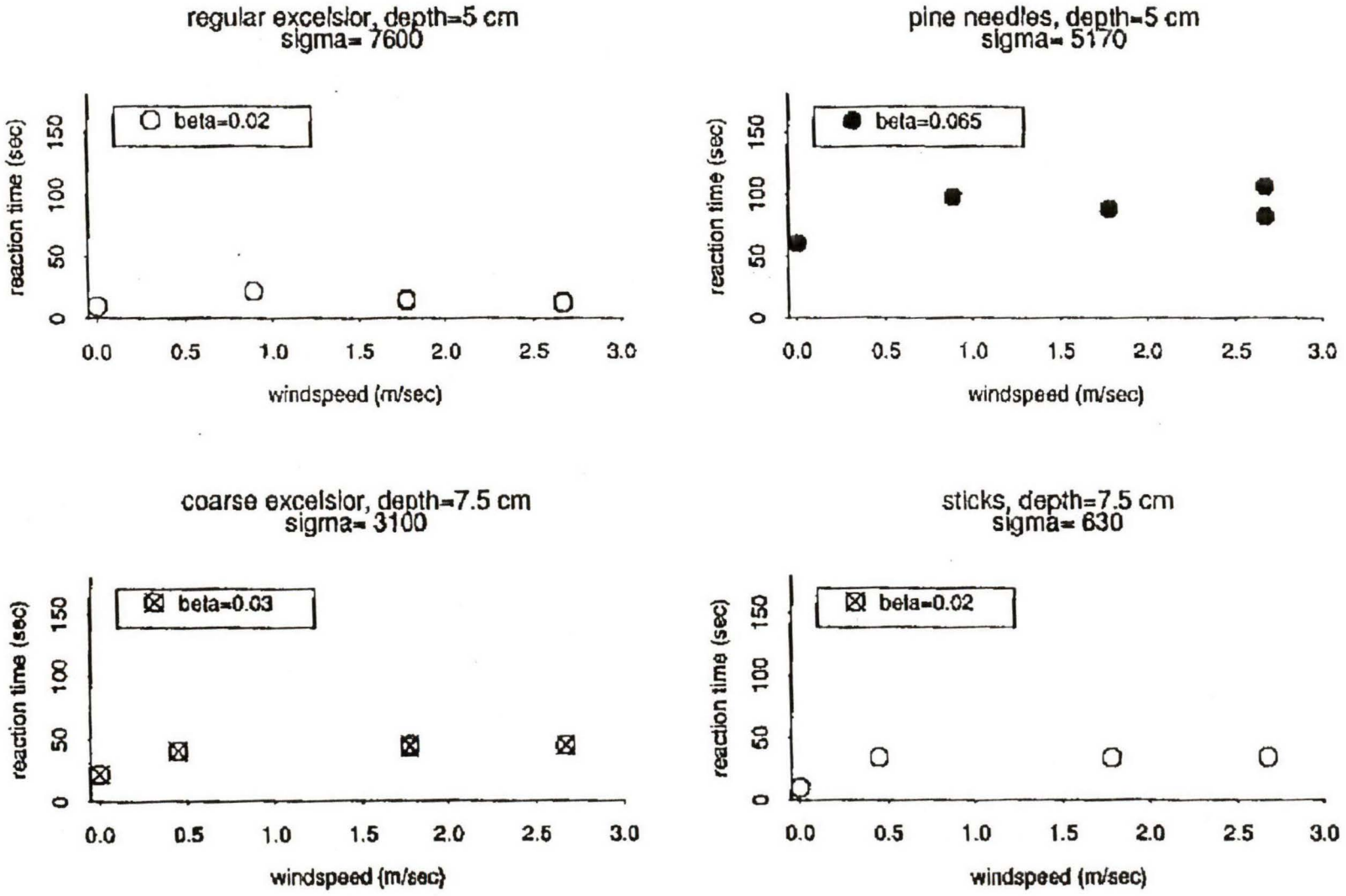

Figure 6

Regular excelsior: reaction time versus moisture content

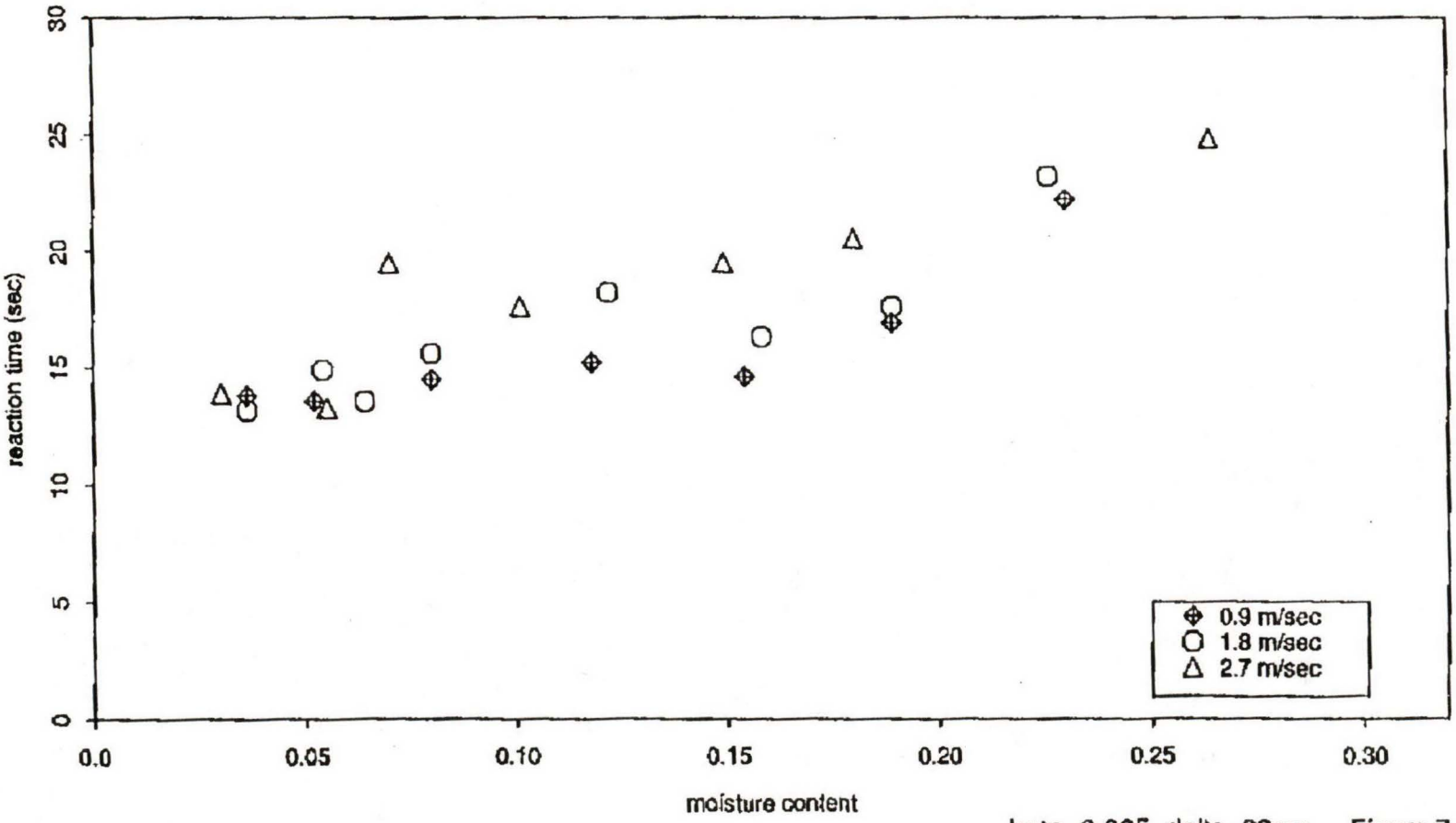

beta=0.005, delta=20cm Figure 7

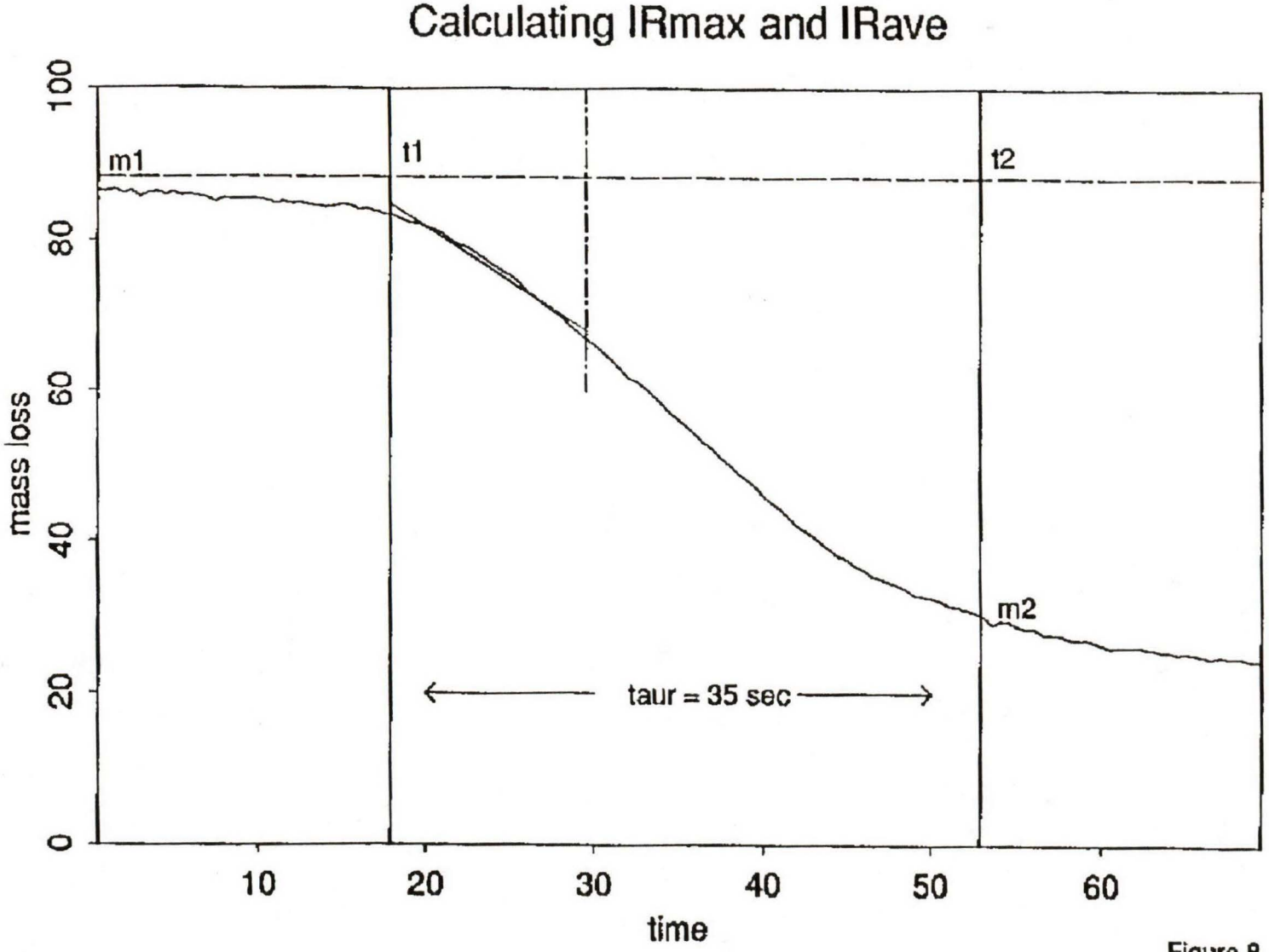
Calculating IRmax and IRave
mass loss
time
m1
t1
t2
m2
taur = 35 sec
0
20
40
60
80
100
10
20
30
40
50
60

Figure 8

Reaction intensity versus windspeed - ambient conditions

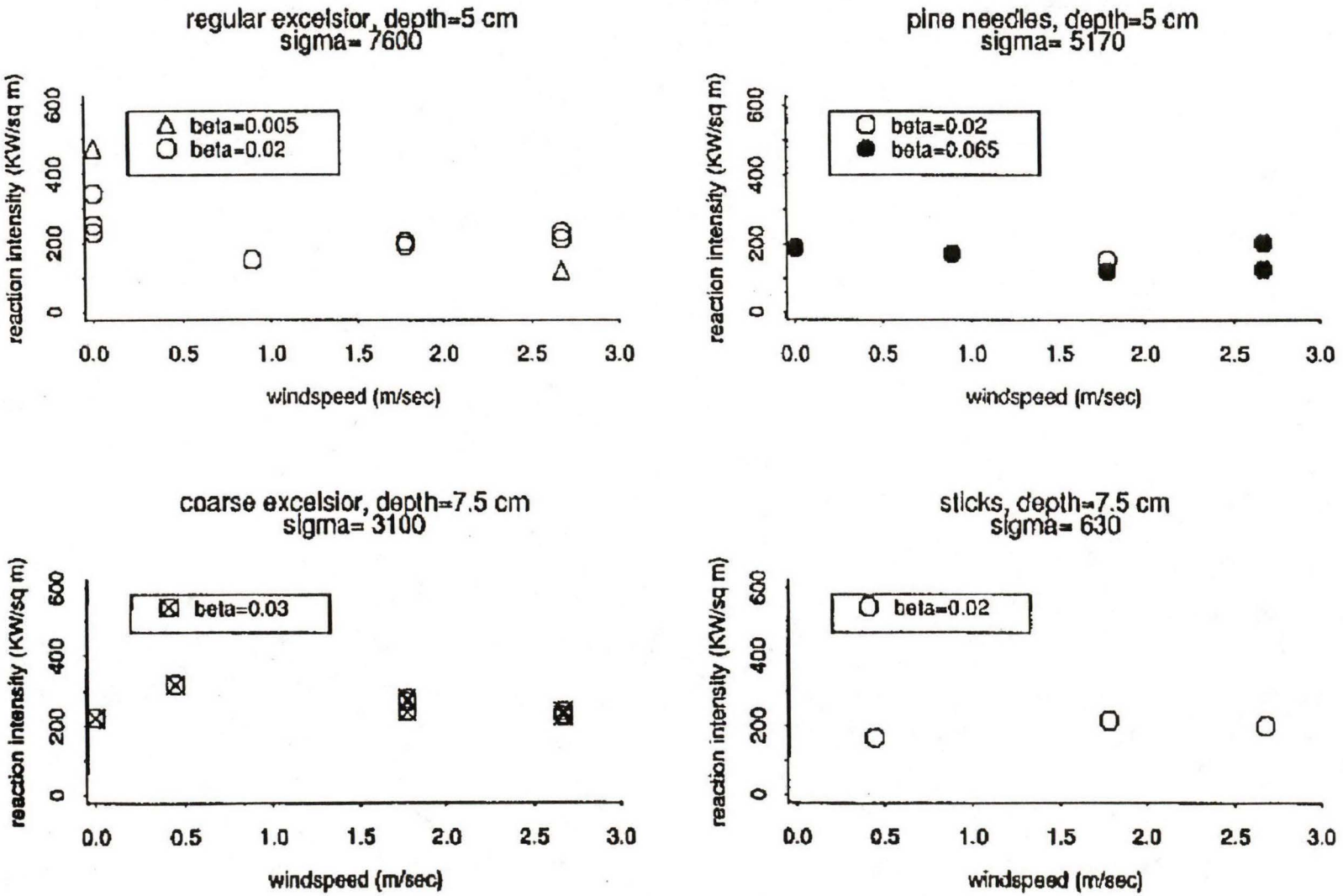

Figure 9

Regular excelsior: reaction intensity versus moisture content

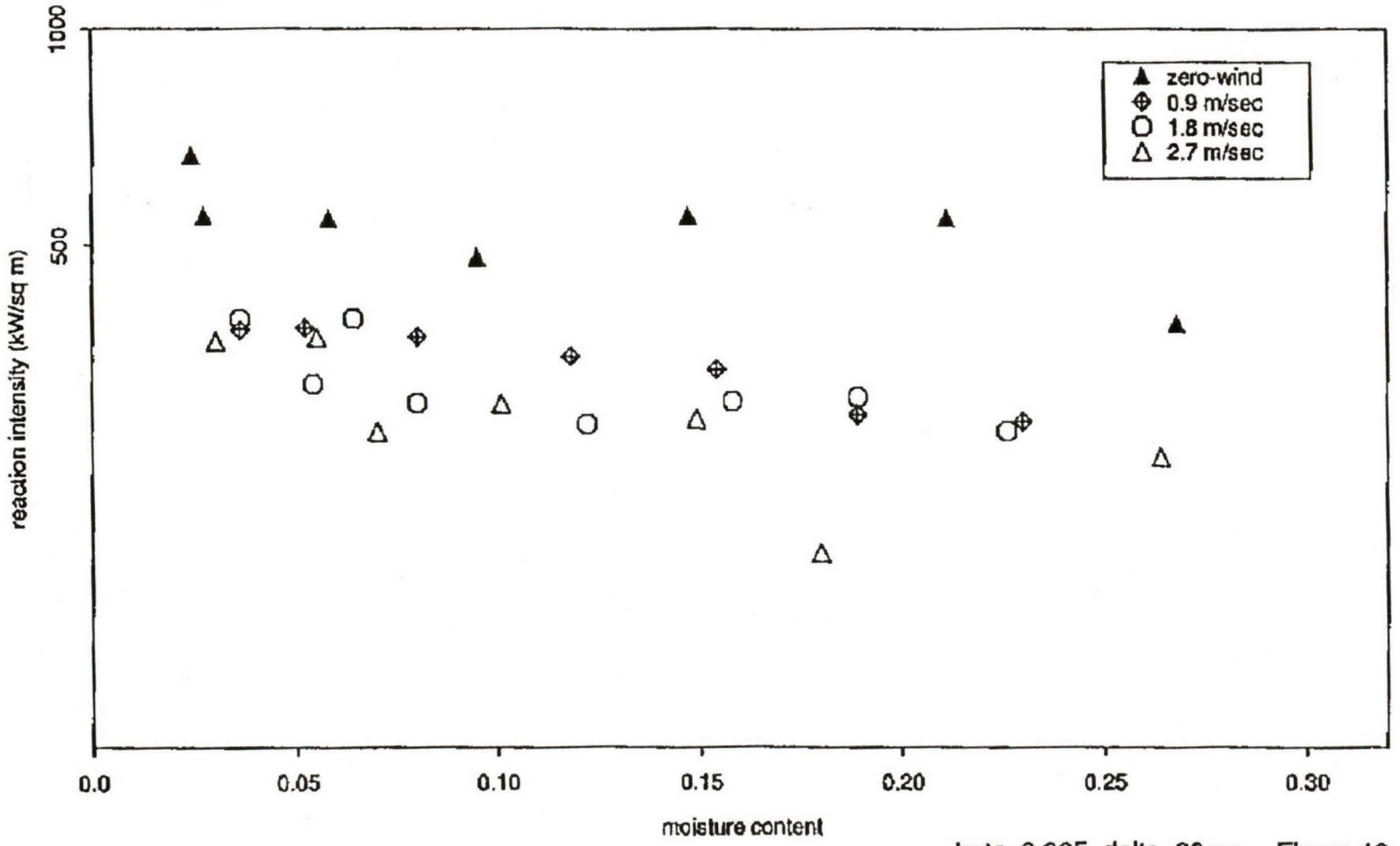

beta=0.005, delta=20cm Figure 10

Fitted reaction intensity for wind-aided fires

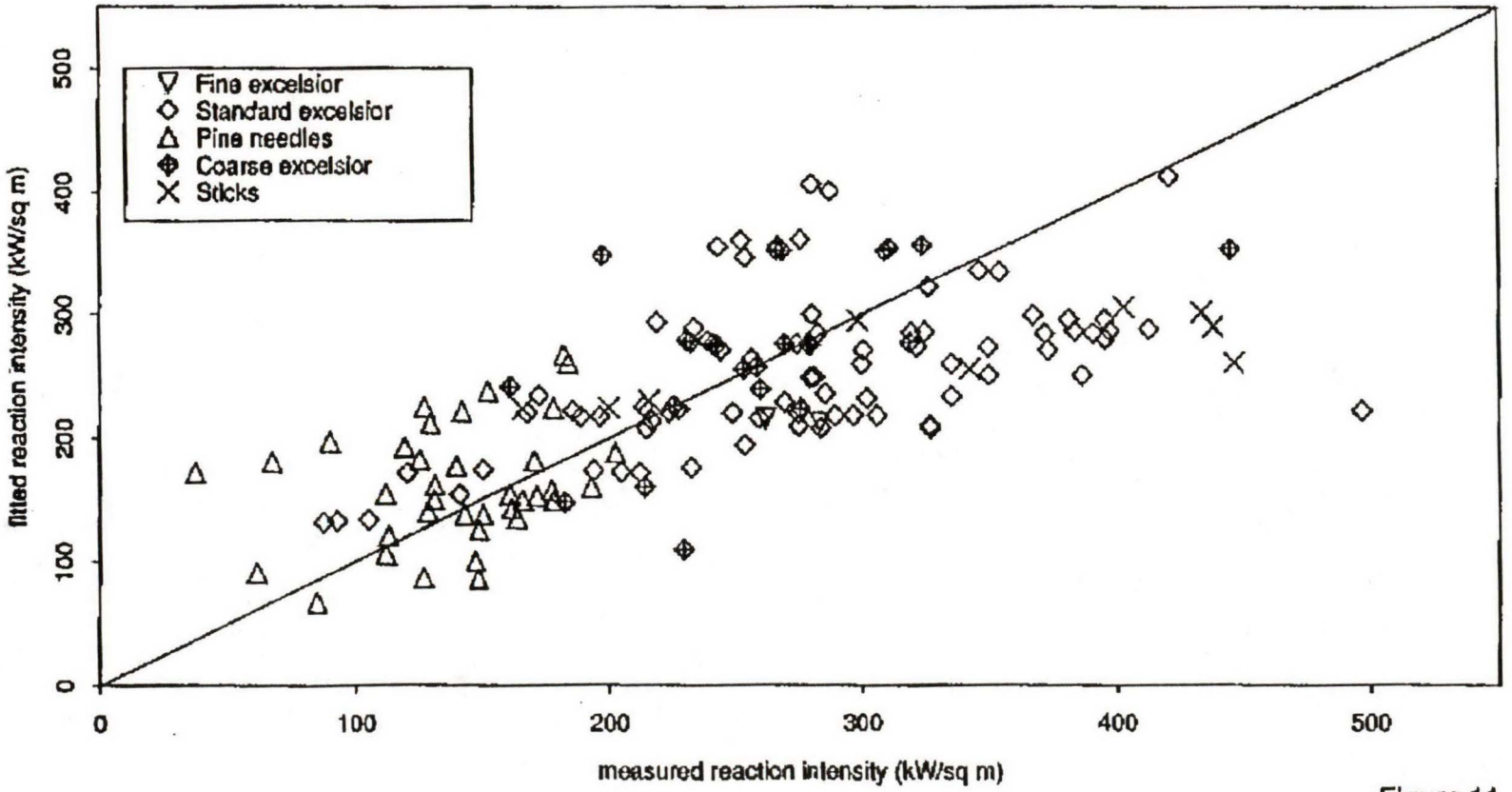

Figure 11

Flame length correlations for wind-aided fires

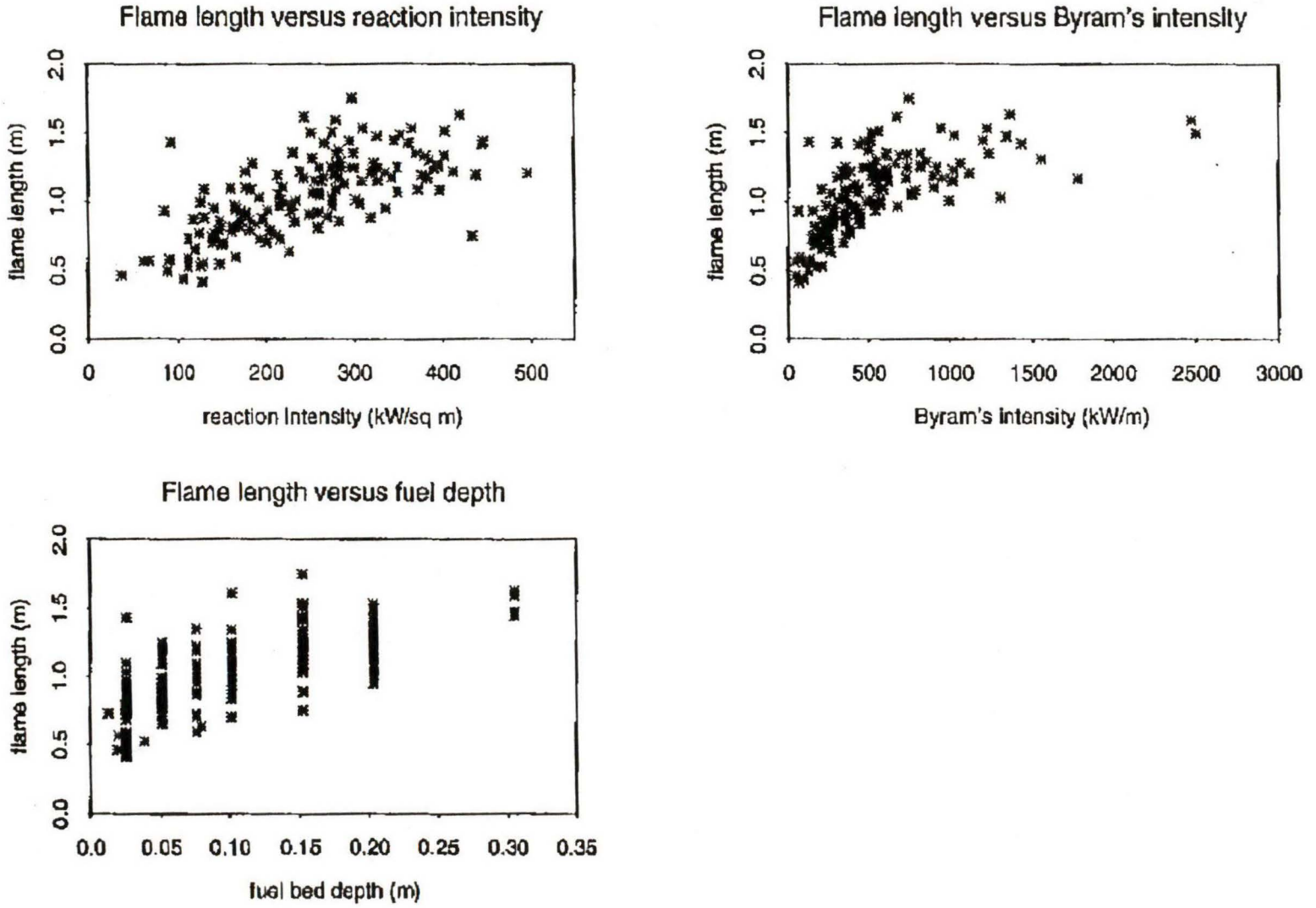

Figure 12

Predictions from Nelson and Adkin's model

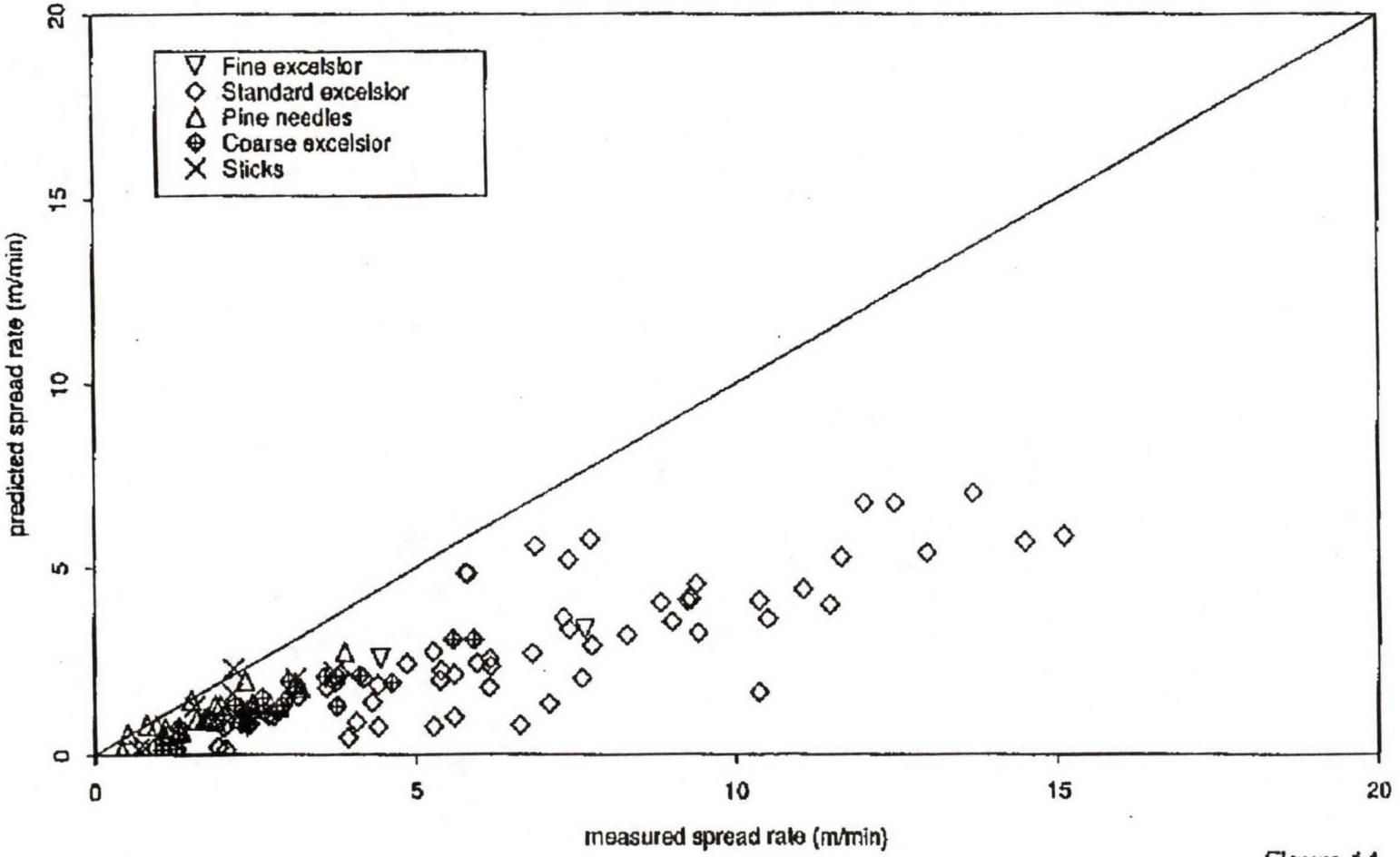

Figure 14

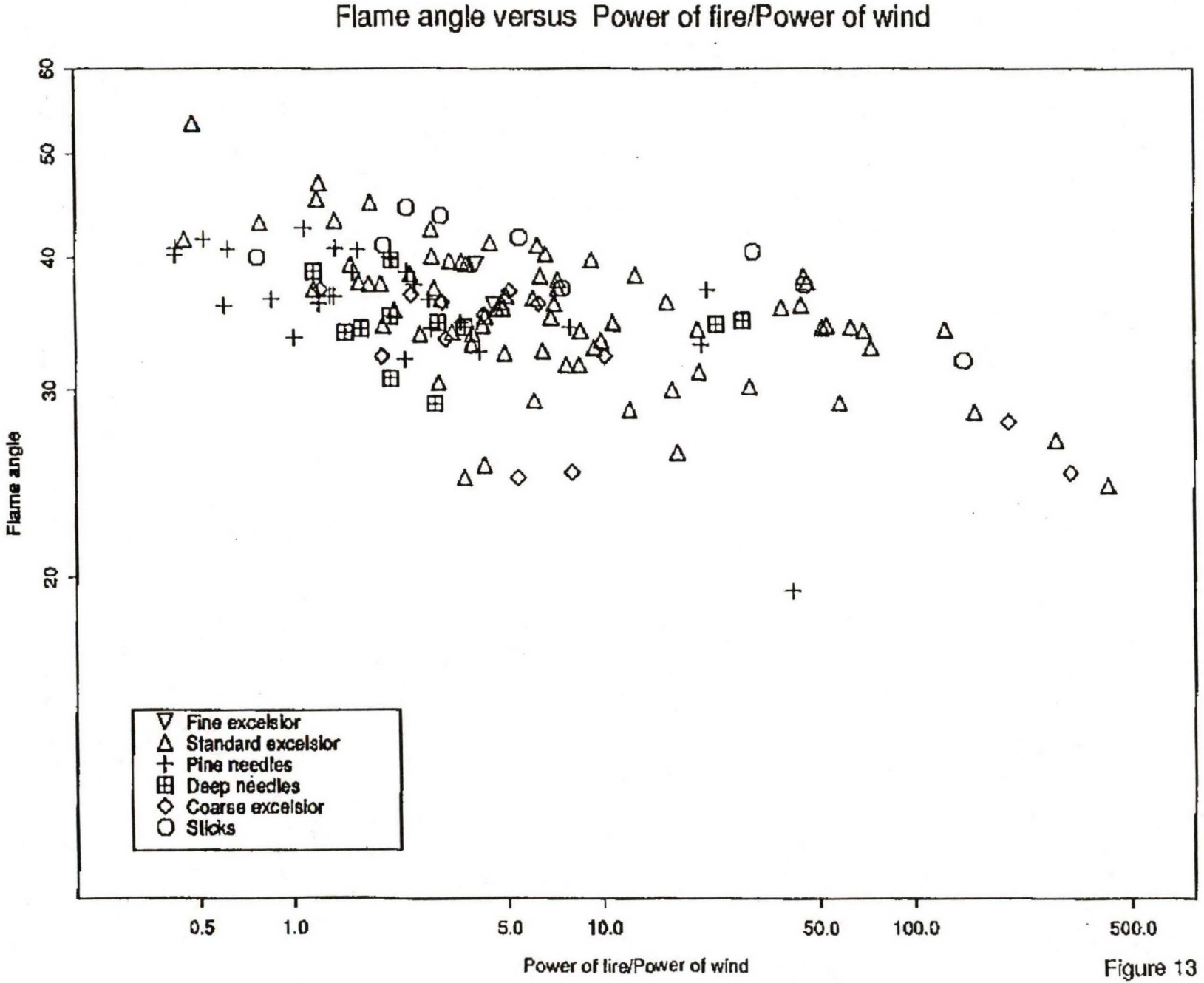
Flame angle versus Power of fire/Power of wind
Flame angle
60
50
40
30
20
0.5
1.0
5.0
10.0
50.0
100.0
500.0
Power of fire/Power of wind
Fine excelsior
Standard excelsior
Pine needles
Deep needles
Coarse excelsior
Sticks

Figure 13